Induced α-Helix Structure in the Aryl Hydrocarbon Receptor Transactivation Domain Modulates Protein−Protein Interactions†

Kate Watt,‡ Thomas J. Jess,§ Sharon M. Kelly,§ Nicholas C. Price,§ and Iain J. McEwan*,‡

School of Medical Sciences, Institute of Medical Sciences, University of Aberdeen, Foresterhill, Aberdeen AB25 2ZD, Scotland, U.K., and Institute of Biomedical and Life Sciences, Joseph Black Building, University of Glasgow, Glasgow G12 8QQ, Scotland, U.K.

Received June 14, 2004; Revised Manuscript Received October 26, 2004

ABSTRACT: The aryl hydrocarbon receptor (AhR) is an intracellular receptor protein that regulates gene transcription in response to both man-made and natural ligands. A modular transactivaton domain (TAD) has been mapped to the 304 C-terminal amino acids and consists of acidic, Q-rich, and P/S/T-rich subdomains. We have used steady-state intrinsic tryptophan fluorescence and circular dichroism spectroscopy to investigate the conformation of the acidic Q-rich region. The results reveal that this region of the protein is structurally flexible but adopts a more folded conformation in the presence of the natural osmolyte trimethylamine *N*-oxide (TMAO) and the solvent trifluoroethanol (TFE). In protein−protein interaction studies, the acidic Q-rich region bound to components of the general transcription machinery [TATA-binding protein (TBP), TAF4, and TAF6] as well as the coactivator proteins SRC-1a and TIF2. The binding site for TBP mapped to the acidic subdomain, while SRC-1a bound preferentially to the Q-rich sequence. Significantly, the binding of TBP was modulated by induced folding of the TAD with TMAO. The results indicate that the AhR TAD makes multiple interactions with the transcriptional machinery and protein conformation plays a critical role in receptor function. Taken together, these findings support a role for protein folding in AhR action and suggest possible mechanisms of receptor-dependent gene activation.

The arylhydrocarbon receptor (AhR)[1] is an intracellular receptor protein that is important for the regulation of genes involved in xenobiotic metabolism and developmental processes (*1*−*3*). The AhR has been shown to induce gene expression in response to toxins such as TCDD (2,3,7,8-tetrachlorodibenzo-*p*-dioxin) as well as natural compounds such as indolo[3,2-*b*]carbazole (ICZ) (*2*, *4*, *5*). When the ligand binds, the AhR dissociates from a complex with hsp 90, heterodimerizes with the AhR nuclear translocator protein (ARNT), and binds to specific DNA sequences termed xenobiotic response elements (XREs), consisting of the minimal five-nucleotide GCGTG motif and flanking residues (*2*, *3*, *6*).

The receptor is characterized by a basic helix−loop−helix (bHLH) DNA binding and dimerization domain at the N-terminus; a second region important for dimerization adjacent to the bHLH is termed the PAS domain, after the proteins Period-ARNT-Single-minded (*7*, *8*). Within the C-terminus of the protein lies a modular transactivation domain (TAD). The importance of the sequences within the 280 C-terminal amino acids of the mouse AhR for transactivation was highlighted using chimeric proteins containing either the glucocorticoid receptor (*9*) or the yeast Gal4 (*10*−*12*) DNA binding domains. Subsequent studies with both the mouse and human receptors have delineated a clear modular structure for the TAD. Three distinct subdomains have been described: an acidic region (amino acids 545−600), a glutamine (Q)-rich region (amino acids 600−713), and a P-, S-, and T-rich sequence (amino acids 713−848) (Figure 1A; *11*, *13*). Varying levels of activity have been reported for the individual regions, while combining the individual domains led to significantly higher levels of transcriptional activation, consistent with synergistic activity between the subdomains in both mammalian cells (*11*, *12*) and the yeast *Saccharomyces cerevisiae* (*13*). In addition, a chimeric activator consisting of the acidic and Q-rich domains fused to the LexA DNA-binding domain activated reporter gene activity under cell-free conditions (*13*). Thus, this region of the protein has been shown to be essential for gene expression and is likely to make both direct and indirect protein−protein interactions with the transcriptional machinery.

† The early stages of this work were funded by a small project grant from the Royal Society (RSRG19571). We also thank the Biotechnology and Biological Sciences Research Council of the United Kingdom for support of the CD facility.

* To whom correspondence should be addressed: School of Medical Sciences, Institute of Medical Sciences, University of Aberdeen, Foresterhill, Aberdeen AB25 2ZD, Scotland, U.K. Telephone: +44-(0)1224−555807. Fax: +44(0)1224-555844. E-mail: iain.mcewan@abdn.ac.uk.

‡ University of Aberdeen.

§ University of Glasgow.

[1] Abbreviations: AhR, arylhydrocarbon receptor; ARNT, arylhydrocarbon receptor nuclear translocator; CBP, CREB-binding protein; ICZ, indolo[3,2-*b*]carbazole; RIP140, receptor interacting protein (140 kDa); SRC-1a, steroid receptor coactivator 1; TAD, transactivation domain; TAF, TBP-associated factor; TBP, TATA-binding protein; TCDD, 2,3,7,8-tetrachlorodibenzo-*p*-dioxin; TIF2, transcription intermediary factor 2; TFE, trifluoroethanol; TMAO, trimethylamine *N*-oxide; XRE, xenobiotic response element.

10.1021/bi0487701 CCC: $30.25
Published on Web 12/13/2004

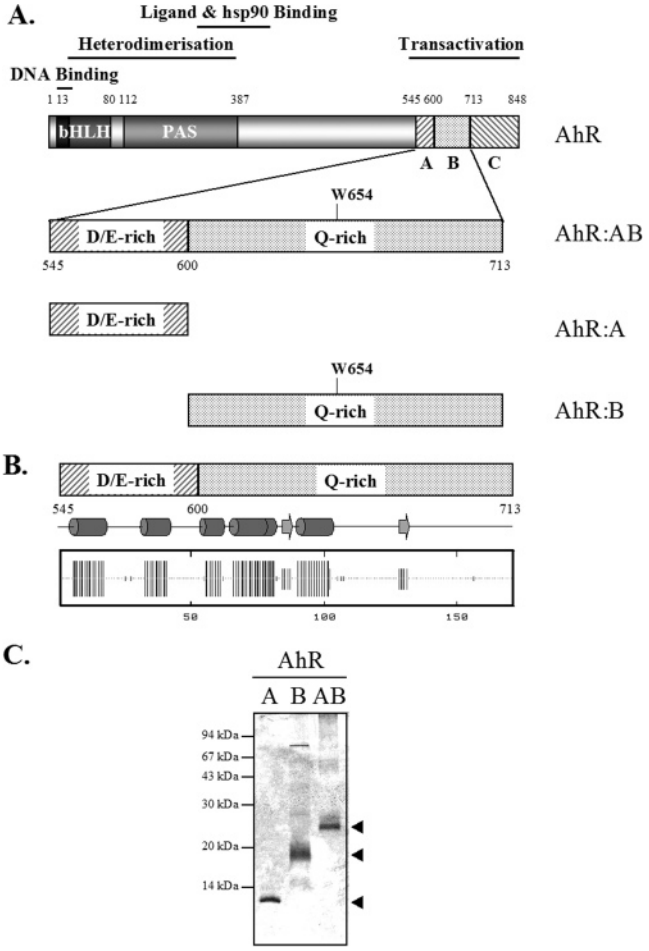

FIGURE 1: (A) Schematic representation of the human AhR, showing the regions of the protein that are important for DNA binding (bHLH, basic helix−loop−helix), heterodimerization with ARNT (PAS domain), ligand binding, and transactivation (refs *2*, *3*, and *11* and references therein). The isolated acidic (A, amino acids 545−600) and Q-rich (B, amino acids 600−713) subdomains are also highlighted, together with tryptophan 654. Region C (amino acids 713−848) represents the proline-, serine-, and threonine-rich subdomain. (B) Secondary structure predictions for the AhR−AB polypeptide, showing putative α-helical (tall bars) and β-strand segments (short bars). The consensus secondary structure prediction was obtained from NPS@ (Network Protein Sequence Analysis, http://pbil.ibcp.fr/NPSA) (*45*). (C) Coomassie-stained gel of purified AhR−A, −B, and −AB polypeptides.

In addition to directly regulating gene expression via XRE sequences, there is growing evidence of cross-talk between the AhR and other signaling pathways, most notably with the estrogen receptor (ER). Thus, the isolated subdomains of the AhR TAD inhibited ER-dependent transcription, while the ER ligand binding domain similarly "squelched" gene activation by the AhR (*14*). This mutual inhibition of activity was taken as evidence that both receptors compete for limiting pools of coregulatory proteins. A direct interaction between the AhR and the ER has also been demonstrated (*15*−*17*). Ohtake *et al*. (*17*) demonstrated a trimolecular complex involving the AhR−ARNT complex and the unliganded ER formed on estrogen response element sequences that resulted in recruitment of the coactivator protein p300 and activation of transcription. The interaction with the ER involved the amino-terminal AF1 transactivation function. In contrast, estradiol-dependent transcription was inhibited by the binding of the AhR−ARNT complex (*17*). These studies would support a role for the AhR in modulating ER signaling either directly or indirectly via the binding of coregulatory proteins.

In contrast to the bHLH and to a lesser extent the PAS domain, little is known about the structure of the TAD. To understand better the role of the AhR in transcription initiation, we have identified possible target proteins within the transcription machinery and examined the folding of the transactivation domain. These studies have revealed a number of protein−protein interactions involving the AhR TAD and general transcription factors and known coregulatory proteins. Structural analysis of the acidic Q-rich subdomains of the AhR TAD revealed a polypeptide with flexible structure that was lost upon incubation with 6 M urea, but adopted a more folded conformation, rich in α-helix structure, in the presence of the structure-stabilizing natural osmolyte trimethylamine *N*-oxide (TMAO) and the solvent trifluoroethanol (TFE). Interestingly, induced folding of the AhR TAD modulated the binding of the general transcription factor, the TATA-binding protein (TBP).

EXPERIMENTAL PROCEDURES

Plasmids. The plasmid pET-AhR−AB, representing amino acids 545−713 of the human AhR, has been described previously (*13*). Plasmids for expressing the acidic and glutamine (Q)-rich subdomains were constructed as follows. The DNA encoding the acidic region (amino acids 545−600) was amplified by PCR using the plasmid phuAhR (a gift from C. Bradfield, Northwestern University, Evanston, IL) as template DNA and the following primers: forward, 5′-GCGCGCGAGCTCTCTAGGCATTGATTTTGAAGA-CAT-3′; and reverse, 5′-GCGCGCGAGCTCATATAATCT-GAAGGTATGAAGGGA-3′. The resulting PCR fragment was subcloned into pET-19bm to generate pET-AhR−A and checked by sequencing. pET-AhR−B encoding the Q-rich subdomain (amino acids 600−713) was constructed as described above using the following primers: forward, 5′-GCGCGCGAGCTCTCAACAGCAACAGTCCTTGGCTC-3′; and reverse, 5′-GCGCGCGAGCTCATTTTGGAATGT-TGTGGTAATACA-3′.

Expression and Purification of Recombinant Proteins. The transactivation domain (TAD) of the human AhR (amino acids 545−713) was expressed in *Escherichia coli* strain BL21(pLys) by induction with 1 mM IPTG for 90 min at 37 °C. Cells were harvested by centrifugation and lysed by freezing and thawing and lysozyme (0.5 mg/ml) treatment, and the recombinant AB fragment was purified from the soluble and insoluble fractions by Ni−NTA agarose affinity chromatography. For the insoluble protein, after cell lysis and centrifugation, the pellet was resuspended in buffer A [10 mM Tris-HCl (pH 8.0), 8 M urea, and 0.1 mM NaH_2PO_4 (adjusted to pH 8 with NaOH)] and stirred slowly at room temperature for 60−90 min. After centrifugation, the supernatant was loaded directly onto a Ni−NTA column which had been equilibrated with buffer A. The column was washed with 5 column volumes of buffer A followed by 10 column volumes of buffer B (like buffer A but with the pH adjusted to 6.3). Bound proteins were eluted with 3 × 1 mL of buffer C (like buffer A but with the pH adjusted to 5.9) followed by 3 × 1 mL of buffer D (like buffer A but with the pH adjusted to 4.5). Purified proteins were dialyzed

against 25 mM HEPES (pH 7.9), 100 mM sodium acetate, 5% glycerol, and 1 mM DTT containing 8 M urea which was reduced stepwise with each change of dialysis buffer until no urea was present. Subdomains A and B were purified from the soluble fraction. The concentrations of all purified proteins was estimated by the Bradford assay using BSA standards and run on 12.5% SDS−acrylamide gels to verify purity (Figure 1C).

Fluorescence Spectroscopy. Fluorescence measurements of purified AhR−AB and AhR−B polypeptides at a concentration of 50 μg/mL in dialysis buffer were taken with a Shimadzu-1501 spectrofluorimeter with excitation and emission bandwidths of 10 nm, using a cuvette with a path length of 1 cm. The fluorescence spectra were measured at excitation wavelengths of both 278 and 295 nm over an emission wavelength range of 300−400 nm. Quenching experiments were carried out in the presence of increasing amounts of acrylamide in the absence and presence of 3 M trimethylamine *N*-oxide (TMAO). As a control, the fluorescence spectrum of NATA (*N*-acetyl-L-tryptophanamide) was also measured in the absence and presence of 3 M TMAO, after excitation at 295 nm. The Stern−Volmer constant (K_{sv}) was calculated using the equation $F_0/F = 1 + K_{sv}[Q]$, where F_0 and F are the fluorescence in the absence and presence of quencher, Q, respectively (*18*). All chemicals were made up in dialysis buffer, and all spectra were corrected for the influence of dialysis buffer.

Circular Dichroism Spectroscopy. Purified AhR−AB (soluble and refolded), −A, and −B polypeptides were dialyzed against 4 mM NaH_2PO_4, 6 mM Na_2HPO_4, 100 mM sodium sulfate, and 1 mM dithiothreitol (pH 7) for CD analysis. The far-UV CD spectra for each protein were measured at 20 °C on a Jasco J-810 spectropolarimeter calibrated with (1*S*)-(+)-10-camphorsulfonic acid. Far-UV CD spectra (195−260 nm) were measured at concentrations in the range of 0.3−0.5 mg/mL using a cell with a path length of 0.02 cm. The far-UV CD spectra for AhR−AB polypeptides were also measured in the presence of 50% trifluoroethanol or 3 M TMAO. Secondary structure analysis was performed by the CONTIN (*19*) method using the DICHROWEB platform available from Birbeck College (University of London, London, England, http://www.cryst.bbk.ac.uk/cdweb/html/) (*20*).

Proteolysis Assay. The purified His-tagged recombinant AhR−AB protein (50 pmol) was digested with trypsin (0.25 ng) or chymotrypsin (2 ng) for 0, 2, 5, 10, and 20 min in the absence or presence of 2 M TMAO. Digestion was carried out at room temperature with or without prior incubation of the protein and TMAO for 30 min at 4 °C, in the presence of 20 mM HEPES (pH 7.9), 10% glycerol, 0.2 mM EDTA, 5 mM $MgCl_2$, 20 mM $CaCl_2$, and 60 mM KCl. Reactions were stopped by the addition of SDS sample loading buffer and heating at 75 °C for 5 min. Fragments were resolved on SDS−polyacrylamide gels, transferred to nitrocellulose, and probed with an anti-histidine antibody (Sigma). The artificial trypsin substrate N^{α}-benzoyl-L-arginine ethyl ester (0.23 mM) was incubated with 0.25 ng/μL trypsin in 63 mM sodium phosphate and 0.06 mM HCl in the presence (1−3 M) or absence of TMAO, and the products of the reaction were assessed by the absorbance at 253 nm.

Protein−Protein Interaction Studies. Purified recombinant AhR−AB, −A, or −B polypeptides (100 nM) in binding buffer (20 mM HEPES, 100 mM KCl, 10% glycerol, 5 mM $MgCl_2$, 0.2 mM EDTA, 0.2 mM PMSF, and 5 mM 2-mercaptoethanol) were adsorbed to the surface of scintillation coated micro-titer plate wells at 4 °C for 72 h; control wells were treated with 100 nM BSA. All wells were subsequently blocked with 5 mg/mL BSA in binding buffer overnight and after removal of the blocking solution incubated with radiolabeled basal transcription factors (TBP and TFIIB), TATA-binding protein-associated factors (TAFs) TAF4, -6, and -9 (*Drosophila* $TAF_{II}110$/human $TAF_{II}130$, *Drosophila* $TAF_{II}60$/human $TAF_{II}80$, and *Drosophila* TAF_{II}-40/human $TAF_{II}32$, respectively; for the unified nomenclature, see ref *21*), co-activators (SRC-1a, TIF2, and CBP), or the corepressor RIP140. Proteins were synthesized and radiolabeled using the Promega rabbit reticulocyte TNT-coupled *in vitro* transcription/translation system. Wells were thoroughly washed with binding buffer containing 1 mg/mL BSA, and the bound radioactivity was measured directly in a micro-β-counter. In some experiments, the bound proteins were stripped from the wells with SDS sample buffer and analyzed by SDS−PAGE and autoradiography.

RESULTS

Protein−Protein Interactions. To regulate target gene expression, the AhR is likely to make multiple interactions with the transcriptional machinery. General transcription factors the TATA-binding protein (TBP), TFIIF (*13*), and TFIIB (*22*) have previously been identified as binding targets for the receptor. In addition to general transcription factors, acidic and Q-rich activators have been reported to interact with subunits of the TFIID protein complex, which consists of TBP and up to 13 TBP-associated factors (TAFs) (refs *23* and *24* and references therein). To further understand AhR−AB function, we have extended the screen for binding partners to other components of the transcriptional machinery, as well as known co-activator or corepressor proteins, and have mapped interactions within the isolated acidic (AhR−A) and Q-rich (AhR−B) subdomains. Figure 2 (panels A and B) confirms the interaction with the TBP and also shows interactions with TAF4 and TAF6, other components of the TFIID complex. Under these conditions, TAF9 shows no significant interaction with the AhR−AB polypeptide. The properties of the AhR−AB polypeptide purified from the soluble fraction of bacterial proteins and from inclusion bodies by urea extraction and refolded *in vitro* were also compared. Virtually the same levels of TBP binding were observed no matter the method of AhR−AB purification (Figure 2C). In mapping studies, it was found that TBP bound preferentially to the acidic subdomain (AhR−A) (Figure 2C). In contrast, binding of TAF4 and -6 was inhibited with both the A and B subdomains compared with AB, and there was no evidence of a preference for either region (data not shown). This suggests a feature of the AhR−AB polypeptide or the interface of the acidic and Q-rich subdomains is important for binding. The result was unexpected for TAF4, as this protein has previously been characterized as a target for Q-rich activators (ref *23* and references therein).

In addition to direct interactions with the transcriptional machinery, the AhR has been reported to bind coregulatory proteins (see the Discussion). We have investigated interactions with a number of well-characterized coactivator proteins

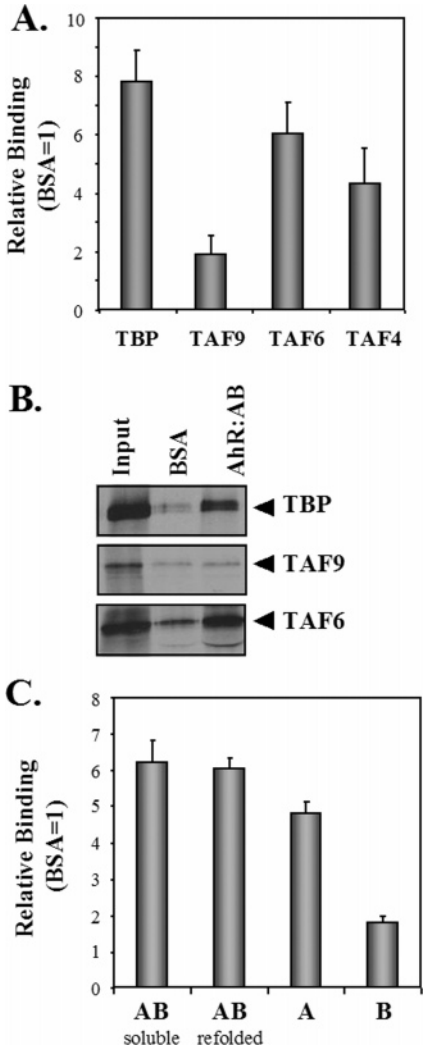

FIGURE 2: Protein−protein binding study of interactions with the TFIID complex. (A) Radiolabeled TBP, TAF4, TAF6, and TAF9 were incubated with the AhR−AB polypeptide or a BSA only control. The binding to BSA was set at 1, and the relative binding that is plotted represents the mean ± standard deviation for four independent measurements. (B) SDS−polyacrylamide gel showing 10% of the starting material (Input) and the recovery of TBP, TAF6, and TAF9 bound to the BSA control or the AhR−AB polypeptide. (C) Radiolabeled TBP was incubated with the AhR−AB (soluble and refolded protein), AhR−A, or AhR−B polypeptide or a BSA only control. The binding to BSA was set at 1, and the relative binding that is plotted represents the mean ± standard deviation for triplicate measurements.

that have been shown to be important for members of the steroid receptor family of ligand-activated transcription factors. A strong interaction was observed for the binding of the p160 protein SRC-1a (Figure 3A). Interestingly, a second member of the p160 family, TIF2, was found to bind less well, while RIP140 and the 1286 N-terminal amino acids of the CREB-binding protein (CBP) exhibited little or no binding under these conditions (Figure 3A). The binding of SRC-1a was mapped predominantly to the Q-rich subdomain of the AhR−AB polypeptide (Figure 3B). Although RIP140 has previously been reported to bind to AhR (*25*), in our hands no significant binding was observed even with the isolated A and B domains (Figure 3B). The binding of SRC-1a was characterized further by mapping the binding of the AhR−AB polypeptide to the CTD (amino acids 977−1441) (Figure 3C,D). Taken together, the studies described above reveal that the AhR TAD is capable of making both direct (TBP, TAF4, and TAF6) and indirect (SRC-1a and TIF2) interactions with the cell transcriptional machinery. The acidic and Q-rich subdomains of the AhR TAD play an important and selective role in these interactions.

Conformational Analysis of the AhR Acidic and Q-Rich Subdomains. In the absence of a high-resolution structure, we have investigated the conformation of the modular AhR TAD using secondary structure predictions, fluorescence and circular dichroism spectroscopy, and sensitivity to protease digestion to examine the conformational properties of this region of the protein. Secondary structure prediction analysis suggests that the acidic subdomain of the AhR TAD is likely to contain two α-helices; the N-terminal half of the Q-rich region is also relatively helical in nature, and the C-terminal part appears to lack defined structure (Figure 1A,B). Within the AhR−AB region, there are five tyrosine residues at positions 584, 599, 672, 687, and 696 and a single tryptophan residue at position 654. We have taken advantage of this to measure the intrinsic fluorescence emission spectra for AhR−AB and AhR−B polypeptides. The emission spectrum for tryptophan and tyrosine residues can give information about the folding of a polypeptide and the local structural environment surrounding the tryptophan. In folded proteins, tyrosine emissions are not usually observed as there is energy transfer to tryptophan: this transfer is distance-dependent and can therefore provide information about protein folding. Panels A and B of Figure 4 show the steady-state emission spectra for the AhR−AB polypeptide after excitation at 278 nm (tyrosine and tryptophan excitation) and 295 nm (tryptophan only excitation), respectively. After excitation at 278 nm, the main features observed are a λ_{max} for tryptophan emission at 344 nm (average of 343 ± 2 nm, $n = 7$) and a shoulder at 307 nm for tyrosine (Figure 4A). A similar λ_{max} for tryptophan (average of 344 ± 4 nm, $n = 5$) but no tyrosine shoulder is seen after excitation at 295 nm (Figure 4B). Under the same conditions, the λ_{max} for tryptophan for the isolated AhR−B subdomain showed a modest "blue shift" to 339 nm, suggesting the tryptophan residues may be more buried (data not shown). The tyrosine signal was more obvious after unfolding in urea. Increasing amounts of urea "red shifted" the λ_{max} for tryptophan to 351 nm and resulted in a clear peak for tyrosine emission (Figure 4A). Both these changes are consistent with unfolding of the polypeptide.

In the studies described above, the binding properties of AhR−AB polypeptides appeared to be similar, independent of the method of purification. To determine that the conformation of the refolded TAD was comparable to that of the soluble protein, the fluorescence emission spectra for both polypeptides were measured after excitation at 295 nm. Figure 4B shows that the undialyzed AhR−AB polypeptide had a red-shifted λ_{max} for tryptophan of 353 nm compared with the values of both the soluble and refolded proteins ($\lambda_{max} = 340$ nm). This indicates that the tryptophan is much more solvent exposed in the undialyzed sample, which would be consistent with the protein being in an unfolded state. The emission spectra for the soluble and refolded AhR TAD polypeptides were essentially indistinguishable (Figure 4B) (see also below). Taken together, these results suggest that removal of the denaturant, urea, leads to folding of the AhR−AB polypeptide into a relatively open conformation that is intrinsic to the polypeptide and not a consequence of the purification process.

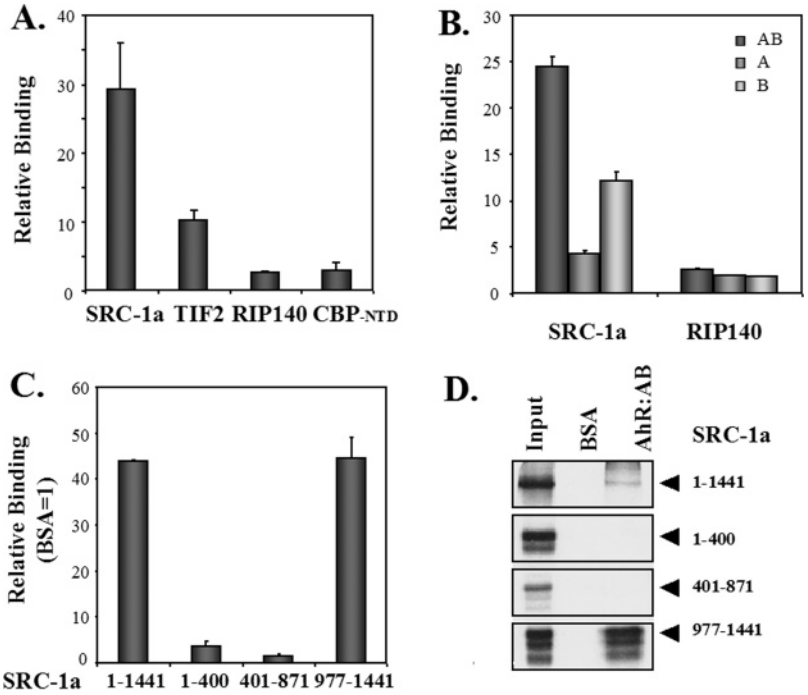

FIGURE 3: Protein−protein binding studies: interactions with coregulatory proteins. (A) Radiolabeled coactivators SRC-1a, TIF2, and CREB-binding protein (CBP, amino acids 1−1286) and the corepressor RIP140 were incubated with the AhR−AB polypeptide or a BSA only control. The binding to BSA was set at 1, and the relative binding that is plotted represents the mean ± standard deviation for at least three independent measurements. (B) Mapping the interactions of SRC-1a and RIP140 with the isolated acidic (AhR−A) and Q-rich subdomains (AhR−B) of the AhR TAD. The binding to BSA was set at 1, and the relative binding to the AhR−A and −B polypeptides represents the mean ± standard deviation for triplicate measurements. (C) Mapping the binding sites for the AhR−AB polypeptide within the SRC-1a coactivator protein. The relative binding of full-length SRC-1a (amino acids 1−1441), NTD (amino acids 1−400), the central region containing LxxLL motifs I−III (amino acids 401−871), and the CTD (amino acids 977−1441) to the AhR−AB polypeptide is shown. The binding to BSA was set at 1, and the relative binding that is plotted represents the mean ± standard deviation for triplicate measurements. (D) After the bound radioactivity had been measured, the wells of the microtiter plate were stripped with SDS sample buffer and the samples analyzed together with 10% of the starting material (Input) by SDS−PAGE. The recovery of the bound full-length and SRC CTD polypeptides is indicated by the arrowheads.

To further investigate the local environment surrounding tryptophan 654, the tryptophan emission was quenched with acrylamide in the absence or presence of 3 M TMAO. TMAO is a natural osmolyte thought to aid in the folding of polypeptides into native conformations (*26*) and has been used successfully to stabilize the folding of the glucocorticoid (*27*) and androgen (*28*, *29*) receptor transactivation domains. The ability of chemicals such as acrylamide to quench the steady-state fluorescence depends on the extent of solvent exposure of the tryptophan residue: tryptophan residues on the surface are more readily quenched than those buried within the protein structure (*18*). Increasing concentrations of acrylamide lead to a progressive reduction of the tryptophan emission in both the presence and absence of TMAO (Figure 5A and data not shown). By plotting the ratio of the fluorescence intensity in the absence (F_o) over the fluorescence intensity in the prescence (F) of quencher against quencher concentration ([Q]), we were able to determine the Stern−Volmer constant (K_{sv}), which gives an indication of the environment of the tryptophan residue (Figure 5B). From the linear plot, a K_{sv} of 8.42 M^{-1} was calculated in the absence of TMAO, consistent with the tryptophan residue being solvent exposed, and a value of 4.65 M^{-1} in the presence of the osmolyte. This reduction in K_{sv} in the presence of TMAO is indicative of the tryptophan being more buried and therefore less exposed to the quenching agent. From these studies, we can conclude that the AhR TAD polypeptide is more folded in the presence of TMAO.

Consistent with this, incubation of the AhR−AB polypeptide with TMAO resulted in a more protease-resistant conformation when challenged with the enzymes chymotrypsin and trypsin. Partial proteolysis with selective protease enzymes has proven to be a useful tool for probing protein conformation. The ability of the protease to cleave will depend on the accessibility of a given site to the enzyme. The AhR−AB polypeptide was incubated with the proteases chymotrypsin and trypsin at 25 °C for increasing amounts of time. Figure 6 shows that in the absence of TMAO the AhR−AB polypeptide is extremely sensitive to digestion with chymotrypsin with no clear ladder of fragments observed and no full-length polypeptide remaining after 5 min. In contrast, in the presence of 2 M TMAO, there was still full-length AhR−AB polypeptide remaining after 20 min, indicating the AhR TAD is more resistant to proteolysis. Similar results were observed with trypsin, which cleaves after basic amino acids, although overall the protein was more resistant to digestion by this enzyme (Figure 6, bottom panel). These results are unlikely due to inhibition of enzyme activity by TMAO, as up to 3 M TMAO did not impair trypsin digestion of the substrate N^{α}-benzoyl-L-arginine ethyl ester (J. Reid and I. J. McEwan, unpublished observations). Taken together, the spectroscopy and partial proteolysis results suggest that the AhR TAD has limited stable structure but adopts a more stable conformation in the presence of TMAO.

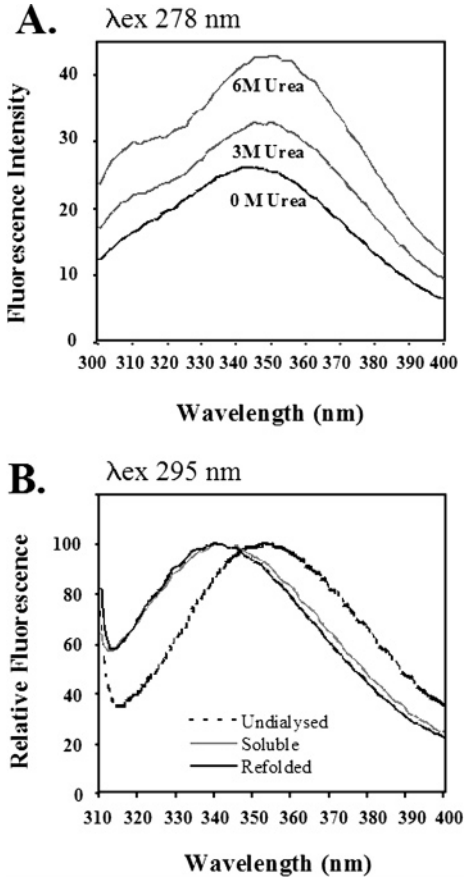

FIGURE 4: Steady-state fluorescence spectroscopy of the AhR−AB polypeptide. (A) Steady-state fluorescence emission spectra for the AhR−AB polypeptide were obtained after excitation at 278 nm in the absence or presence of increasing amounts of urea (0, 3, and 6 M). The spectra that are shown represent the average of duplicate readings, corrected for buffer. The dominant emission peak is from the tryptophan residue, and the shoulder at 307 nm represents tyrosine emission. (B) Steady-state fluorescence emission spectra for the AhR−AB polypeptide were obtained after excitation at 295 nm before (undialyzed) or after (refolded) removal of urea. The emission spectrum for the soluble AhR−AB polypeptide is also shown for comparison. The relative fluorescence intensity is calculated by setting the tryptophan λ_{max} to 100% and is plotted vs wavelength (nanometers). The spectra that are shown are from a representative experiment and are the average of duplicate readings, corrected for buffer.

To determine the secondary structure content of the AhR−AB polypeptide and the A and B subdomains, we measured the far-UV circular dichroism spectrum for each polypeptide. Figure 7A shows the far-UV spectrum for both the soluble and refolded AhR−AB polypeptides. The spectra are very similar and are dominated by the minimum at around 200 nm, which is indicative of polypeptides with significant nonordered structure. Analysis of the secondary structure content revealed a significant amount of β-strand and nonordered structure but relatively little α-helix (Table 1). Analysis of the A and B subdomains also showed proteins with relatively little stable secondary structure (Figure 7B). Significantly, the sum of the A and B spectra was equivalent to the measured spectrum for AB (data not shown), which would suggest the observed spectra reflect the structure of the subdomains within the AhR−AB polypeptide. Interestingly, the observed spectra suggest that the acidic subdomain is less α-helical than the Q-rich region (Figure 7B). Changes in secondary structure content in response to induced folding

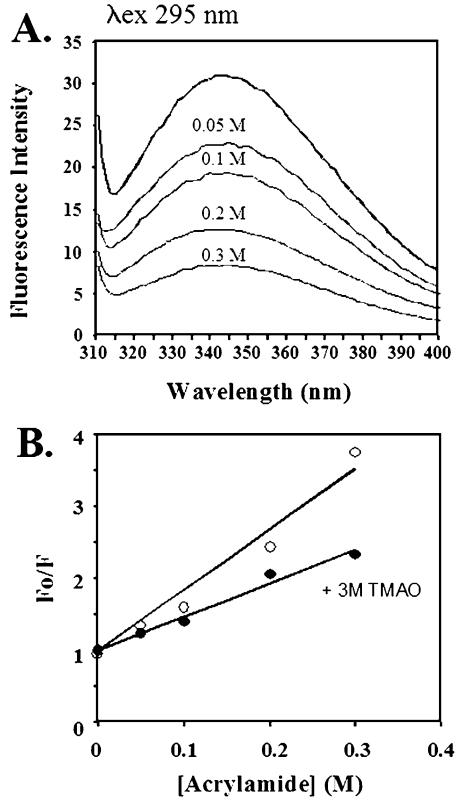

FIGURE 5: Acrylamide quenching of the steady-state fluorescence spectrum of the AhR−AB polypeptide in the absence or presence of 3 M TMAO. (A) Increasing acrylamide quenches the tryptophan fluorescence emission spectra for the AhR−AB polypeptide. Data shown are after excitation at 295 nm, in the absence of TMAO. The spectra that are shown represent the average of duplicate readings, corrected for buffer. (B) Stern−Volmer plots of acrylamide quenching in the absence (○) or presence (●) of 3 M TMAO. F_0 and F represent the fluorescence intensity in the absence and presence of the quencher, respectively.

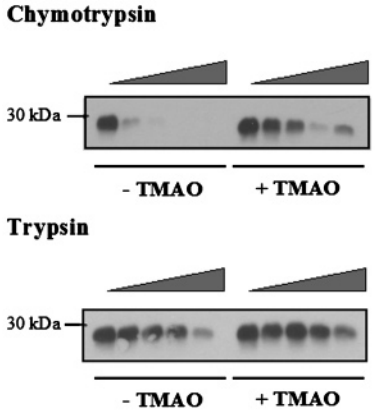

FIGURE 6: Partial proteolysis of the AhR−AB polypeptide. The time-dependent (0, 2, 5, 10, and 20 min) digestion of 50 pmol of the AhR−AB polypeptide with 2 ng of chymotrypsin (top panel) or 0.25 ng of trypsin (bottom panel) is shown. Digestion of the full-length protein was followed by resolving the products of the reaction by SDS−PAGE and transferring them to nitrocellulose. Amino-terminal fragments were then identified using an anti-histidine tag antibody (Sigma) in Western blot analysis. Proteolysis was carried out in the absence (−) or presence (+) of 2 M TMAO.

of the AhR−AB polypetide by the structure-stabilizing agents TFE and TMAO were also determined. Figure 4C shows the far-UV spectra for the AhR−AB polypeptide in buffer (3 M TMAO and 50% TFE). In the presence of both agents,

Table 1: Summary of Secondary Structure Content[a]

protein	α-helix (%)	β-strand (%)	turn (%)	nonordered (%)
soluble AB/buffer	13.4	34.4	21.7	30.5
soluble AB/TFE	48.2	10.3	15	16.5
refolded AB/buffer	12.8	33.7	21.9	31.6
refolded AB/TFE	58.7	5.4	14.9	21

[a] The secondary structure content was determined by the CONTIN method as described in Experimental Procedures. In all cases, the NMRSD (normalized mean root square derivation) between calculated and experimental spectra was in the range of 6−9%.

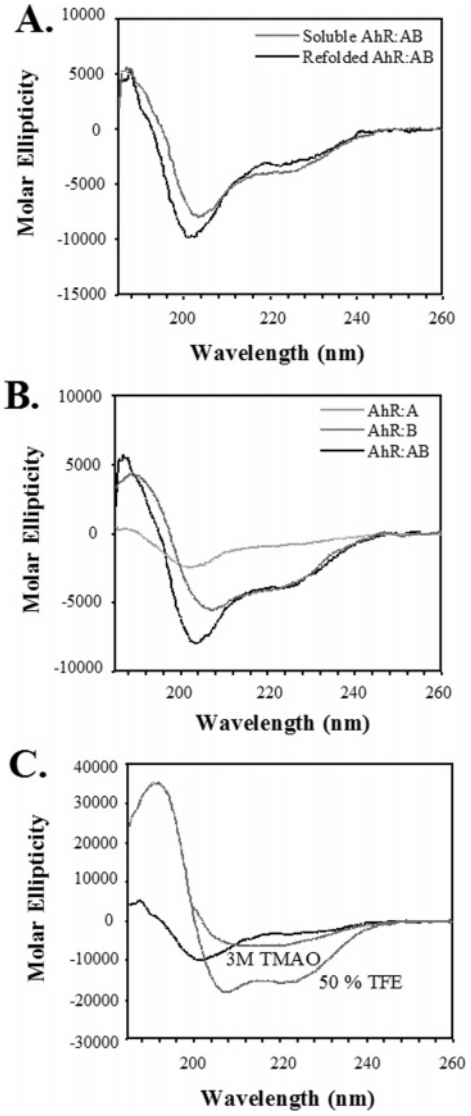

FIGURE 7: CD spectra for probing the secondary structure content within the AhR TAD. (A) Far-UV CD spectra for soluble and refolded AhR−AB polypeptides (gray and black lines, respectively) in phosphate buffer. The minimum at 200 nm is characteristic of a significant contribution of nonordered structure. (B) Far-UV CD spectra for soluble AhR−AB (black line), AhR−A (light gray line), and AhR−B (dark gray line) polypeptides. (C) Far-UV CD spectra for the AhR−AB polypeptide in buffer (black line), 3 M TMAO (gray line), and 50% TFE (gray line). The spectra observed in the presence of TMAO and TFE with minima at ∼208 and ∼222 nm are characteristic of α-helical secondary structure. Similar conformational changes were observed for the refolded AhR−AB polypeptide (Table 1 and data not shown).

there are changes in the spectrum consistent with an increase in α-helix content. There was an increase from 13 to 48−58% in α-helical content in the presence of TFE, at the expense of β-strand, β-turn, and nonordered structure (Table 1). It was not possible to estimate the secondary structure content in the presence of TMAO because of the high absorbance below 210 nm under these conditions. However, taken together, these results indicate that both the soluble and refolded AhR TAD have essentially the same conformation, which adopts an α-helix-rich structure in the presence of TMAO and TFE.

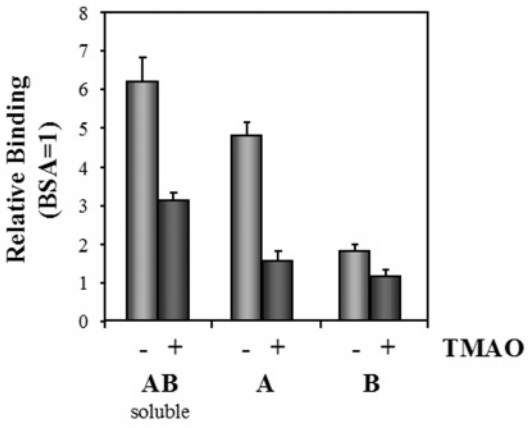

FIGURE 8: Folding of the AhR TAD modulates protein−protein interactions. The isolated AhR−A and −B subdomains or the AhR−AB polypeptide were preincubated in the absence or presence of 2 M TMAO prior to incubation with radiolabeled TBP. Binding was carried out in triplicate, and the binding relative to a BSA only control is shown (mean ± standard deviation).

The structural analysis presented above indicated that the AhR−AB polypeptide had a flexible conformation but adopted a more folded or stable structure in the presence of TMAO. Recently, folding of the glucocorticoid receptor and androgen receptor AF-1 transactivation domains was shown to enhance the binding of coregulatory proteins (*27*, *29*). We therefore investigated the effect of induced folding of the AhR TAD on the binding of TBP. Figure 8 shows that preincubation with 2 M TMAO significantly reduced the level of binding of TBP to both the AhR−AB and −A polypeptides, but as expected had little or no effect on the interaction with the B subdomain. These results support a model whereby the structural flexibility of the TAD is important for the interaction with the general transcription factor TBP.

DISCUSSION

In addition to its well-documented role in the expression of xenobiotic metabolizing enzymes, the AhR is also important for normal development of the liver and immune system. These diverse actions of the AhR are likely to reflect the ability to regulate different patterns of gene expression in a ligand-dependent manner. To understand better the mechanism(s) of receptor-dependent gene regulation, we have studied the structure and function of the acidic and Q-rich sequences in the C-terminal transactivation domain (TAD). Fluorescence emission spectra for endogenous aromatic amino acids and the far-UV CD spectra revealed that the acidic Q-rich subdomains of the AhR TAD are structurally flexible. This region of the protein can be folded into a more stable conformation, rich in α-helix, in the presence of the structure-stabilizing agents TMAO and TFE

or unfolded by the denaturant urea. The acidic region and the amino-terminal end of the Q-rich region are predicted to be α-helical, while the carboxyl-terminal half of the Q-rich subdomain exhibited essentially no predicted secondary structure. However, these predictions were not supported by the CD analysis, which suggested the AhR TAD contained significant *β*-strand and nonordered structure. Recently, Jones and Whitlock (*30*) showed that mutating phenylalanines 542 and 566 (Phe550 and -572, respectively, in the human AhR) to prolines, to disrupt the putative helices in the acidic region, had little effect on transactivation by a chimeric receptor. This led these authors to the conclusion that helical structure was not critical for activity. However, it is not clear that this particular portion of the protein is in fact α-helical, so the mutations may not actually disrupt helical segments in this region, which have been proposed on the basis of secondary structure prediction algorithms. In contrast, mutating phenylalanine 542 and flanking isoleucine residues to alanines dramatically impaired receptor-induced expression of endogenous CYP1A1 mRNA and reporter gene activity, supporting the view that hydrophobic residues play an important role in transactivation (*30*). The unambiguous identification and role of secondary structure elements within the AhR TAD will require further detailed structural analysis of this region of the protein.

Although the TADs from a wide range of both viral and cellular transactivator proteins show little if any sequence homology, they do share a common property in being structurally flexible and adopt a more structured conformation upon specific protein−protein interactions (ref *28* and references therein). From a thermodynamic and functional perspective, this allows for multiple interactions without compromising specificity (reviewed in ref *31*). A further advantage in structural flexibility is that induction of structure through a specific protein−protein interaction may lead to the creation of "new" surfaces that facilitate subsequent interactions and/or alterations to existing interactions. It is striking therefore that induced folding of the AhR TAD or acidic subdomain led to, at least, a 50% reduction in TBP binding. In contrast, induced structure within the androgen receptor AF-1 domain, by TMAO or TFIIF binding, significantly increased the level of binding of the coactivator protein SRC-1a (*29*), while folding of the glucocorticoid receptor AF-1 domain by TMAO enhanced binding to the general transcription factor TBP and coactivator proteins GRIP1 and CBP (*27*). This would suggest that the ability to fold is an important component of certain protein−protein interactions, while other interactions are enhanced by a more folded conformation. It will be interesting to see which, if any, of the protein−protein interactions identified to date can lead to folding of the AhR TAD.

Mapping studies revealed that general transcription factor TBP preferentially bound to the acidic (amino acids 545−600) subdomain. Previously, Metz *et al*. (*32*) described a "TBP-binding motif" (TBM) in the cellular activator c-Fos and viral activators E1A and VP16. Related sequences can be found in other activators reported to bind TBP, including p53, p65 (NF-*κ*B), c-myc, and the glucocorticoid receptor, giving a consensus *ϕϕψ*/F*ψψϕψ*x- sequence, where *ϕ* and *ψ* represent hydrophilic and hydrophobic amino acids, respectively, the hyphen is an acidic residue, and x is any amino acid. Interestingly, there are sequences within the AhR−A subdomain related to the consensus, the best match being ^{579}DEILtyVqD^{587}. This sequence is totally conserved among human, mouse, rat, pig, rabbit, and chicken AhR sequences and falls within the second predicted helical segment of the acidic subdomain. Mutating the hydrophobic residues, I581, L582, and V585, within this region resulted in a reduction in transactivation activity (*30*). Taken together, these findings emphasize the importance of hydrophobic amino acids for TAD structure and/or function and are consistent with the AhR acidic subdomain acting, at least in part, by binding the TBP.

Binding of coactivator protein SRC-1a was mapped to sequences within the Q-rich (amino acids 600−713) subdomain. In the case of SRC-1a, the AhR-binding site was delineated to the 465 C-terminal amino acids, which contain a Q-rich region, a binding site for methyltransferases, and a single LxxLL motif (see refs *33* and *34*). Kumar and Perdrew (*35*) also mapped the binding of SRC-1a to the Q-rich region of the human AhR TAD and, interestingly, implicated the LxxLL motifs of SRC-1a as being important for this interaction. Although the precise motif or motifs involved were not identified, our results would support a role for the very C-terminal LxxLL sequence (motif IV). It is striking therefore that the related p160 coactivator, TIF2, exhibited significantly less binding to the AhR−AB polypeptide than SRC-1a (Figure 3). SRC-1a and TIF2 share three regions with a high degree of homology, including the central "NR boxes" (LxxLL motifs I−III), but TIF2 lacks a corresponding C-terminal LxxLL sequence (motif IV). Taken together, these results would support a role for the C-terminal region of SRC-1a in AhR binding. This region of the coactivator has also recently been shown to bind to the androgen receptor AF-1 domain (*36*). In addition to an LxxLL motif, this part of SRC-1a has a Q-rich region that is important for the interaction with the androgen receptor amino-terminal domain (*37*, *38*). Recently, Hankinson and co-workers (*39*) showed that all three members of the p160 family of coactivators (SRC-1, TIF2, and ACTR) are recruited to the enhancer sequence of the CYP1A1 gene in an AhR/TCDD-dependent manner. Beischlag *et al*. (*39*) also mapped the AhR binding site to sequences in the C-terminus of SRC-1 (amino acids 896−1200). This sequence overlaps the fragment used in this study but lacks the 241 amino acids of the SRC-1a C-terminus, including the LxxLL motif. Thus, while sequences within the C-terminal half of SRC-1a are clearly important for the interaction with the AhR, the fine mapping of the binding site awaits further mutagenesis studies.

In vitro interactions of the coregulator/corepressor protein RIP140 with mouse AhR deletion constructs suggested the TAD is required for binding (*25*). Interestingly, relatively modest binding was observed with the acidic Q-rich region compared with the binding of the Q-rich subdomain alone or constructs containing the proline-, serine-, and threonine-rich subdomain: no binding was detected with the isolated acidic or P-, S-, and T-rich subdomains (*25*). In the study presented here, there was also little binding with the AhR−AB (acidic-Q-rich) or AhR−A (acidic) polypeptides, and somewhat surprisingly, there was no significant binding with the isolated Q-rich region (AhR−B). The reason for this apparent lack of binding is unclear but may simply reflect the different experimental approaches that have been used. A protein involved in chromatin remodeling, BRG-1, has

also been reported to bind to the Q-rich sequence and to cooperate with SRC-1 in regulating reporter gene activity (*40*). Significantly, BRG-1 was shown to be necessary for induction of the endogenous CYP1A1 mRNA and to be recruited to the enhancer sequence in an AhR-, ARNT-, and ligand-dependent manner (*40*). The general transcription factor TFIIB (*22*), the coactivator ERAP140 (*41*), and the corepressor SMRT (*41*) have all been reported to interact with the AhR, but the sequences that are involved remain to be determined. The AhR has recently been shown to interact directly with the cyclin T1 subunit of P-TEFb (positive transcription elongation factor), resulting in protein recruitment to the *cyp1a1* promoter, although the region(s) of the receptor involved remains to be determined (*42*). P-TEFb phosphorylates the C-terminal domain of the large subunit of the RNA polymerase II enzyme, which is important for promoter escape and transcription elongation.

The assembly of protein complexes on target genes is a key regulatory step in transcriptional control. From the above, it is clear that AhR can participate in multiple protein−protein interactions: in this study, we have described multiple interactions between the AhR−AB polypeptide and components of the general transcriptional machinery (TBP, TAF4, and TAF6) and coactivators (SRC-1 and TIF2). Interactions with different targets have previously been described as a likely mechanism for synergism between multiple DNA-bound activators or a single activator with a modular TAD structure (see refs *43* and *44*). An elegant example of the latter is the *Drosophila* Bicoid transcription factor, which possesses glutamine (Q)-rich and alanine-rich subdomains that interact with TAF4 and TAF6, respectively. In a reconstituted *in vitro* transcription assay, synergism from multiple bound Bicoid proteins required both subdomains and the presence of TAF4 and TAF6 in the TFIID complex (*44*). Interestingly, TBP and SRC-1 bound to distinct subdomains of the AhR TAD and thus provides a plausible mechanism for the observed synergy that has been reported for the AhR−AB protein compared with the isolated subdomains (*11*−*13*). Structural analysis revealed that the AhR−AB subdomains are likely to have a flexible conformation that undergoes induced folding in the presence of the natural osmolyte TMAO, which in turn modulated binding of general transcription factor TBP. The latter finding emphasizes the dynamic nature of protein conformation and protein−protein interactions and is an important feature of transactivation domain function. To understand further the mechanism(s) whereby the DNA-bound AhR regulates gene expression, it will be important to consider this interplay between protein conformation and protein−protein interactions.

ACKNOWLEDGMENT

We are grateful to Professor Jan-Åke Gustafsson (Karolinska Institute, Stockholm, Sweden) for the gift of pET-AhR-AB, pET-AhR-A, and pET-AhR-B [the latter plasmid was made by Dr. J. Craig Rowlands (Burdock Group, Vero Beach, FL)]. We also thank Professors R. Goodman (Vollum Institute, Portland, OR), B. W. O'Malley (Baylor College of Medicine, Houston, TX), and M. G. Parker (Imperial College, London School of Medicine, London, England), R. Tjian (University of California, Berkeley, CA) for the gift of plasmids expressing the coregulatory proteins CBP, SRC-1a, RIP140, and TAFs, respectively.

REFERENCES

1. Hankinson, O. (1995) The aryl hydrocarbon receptor complex, *Annu. Rev. Pharmacol. Toxicol. 35*, 307−340.
2. Rowlands, J. C., and Gustafsson, J.-Å. (1997) Aryl hydrocarbon receptor-mediated signal transduction, *Crit. Rev. Toxicol. 27*, 109−134.
3. Whitlock, J. P., Jr. (1999) Induction of cytochrome P4501A1, *Annu. Rev. Pharmacol. Toxicol. 39*, 103−125.
4. Denison, M. S., Pandini, A., Nagy, S. R., Baldwin, E. P., and Bonati, L. (2002) Ligand binding and activation of the Ah receptor, *Chem.-Biol. Interact. 141*, 3−24.
5. Denison, M. S., and Nagy, S. R. (2003) Activation of the aryl hydrocarbon receptor by structurally diverse exogenous and endogenous chemicals, *Annu. Rev. Pharmacol. Toxicol. 43*, 309−334.
6. Swanson, H. I. (2002) DNA binding and protein interactions of the AHR/ARNT heterodimer that facilitate gene activation, *Chem.-Biol. Interact. 141*, 63−76.
7. Gu, Y. Z., Hogenesch, J. B., and Bradfield, C. A. (2000) The PAS superfamily: Sensors of environmental and developmental signals, *Annu. Rev. Pharmacol. Toxicol. 40*, 519−561.
8. Kewley, R. J., Whitelaw, M. L., and Chapman-Smith, A. (2004) The mammalian basic helix-loop-helix/PAS family of transcriptional regulators, *Int. J. Biochem. Cell Biol. 36*, 189−204.
9. Whitelaw, M. L., Gustafsson, J.-Å., and Poellinger, L. (1994) Identification of transactivation and repression functions of the dioxin receptor and its basic helix-loop-helix/PAS partner factor Arnt: Inducible versus constitutive modes of regulation, *Mol. Cell. Biol. 14*, 8343−8355.
10. Jain, S., Dolwick, K. M., Schmidt, J. V., and Bradfield, C. A. (1994) Potent transactivation domains of the Ah receptor and the Ah receptor nuclear translocator map to their carboxyl termini, *J. Biol. Chem. 269*, 31518−31524.
11. Ma, Q., Dong, L., and Whitlock, J. P., Jr. (1995) Transcriptional activation by the mouse Ah receptor. Interplay between multiple stimulatory and inhibitory functions, *J. Biol. Chem. 270*, 12697−12703.
12. Sogawa, K., Iwabuchi, K., Abe, H., and Fujii-Kuriyama, Y. (1995) Transcriptional activation domains of the Ah receptor and Ah receptor nuclear translocator, *J. Cancer Res. Clin. Oncol. 121*, 612−620.
13. Rowlands, J. C., McEwan, I. J., and Gustafsson, J.-Å. (1996) Trans-activation by the human aryl hydrocarbon receptor and aryl hydrocarbon receptor nuclear translocator proteins: Direct interactions with basal transcription factors, *Mol. Pharmacol. 50*, 538−548.
14. Reen, R. K., Cadwallader, A., and Perdrew, G. H. (2002) The sub-domains of the transactivation domain of the aryl hydrocarbon receptor (AhR) inhibit AhR and estrogen receptor transcriptional activity, *Arch. Biochem. Biophys. 408*, 93−102.
15. Klinge, C. M., Kaur, K., and Swanson, H. I. (2000) The aryl hydrocarbon receptor interacts with estrogen receptor α and prphan receptors COUP-TFI and ERRα1, *Arch. Biochem. Biophys. 373*, 163−174.
16. Wormke, M., Stoner, M., Saville, B., Wlker, K., Abdelrahim, M., Burghardt, R., and Safe, S. (2003) The aryl hydrocarbon receptor mediates degradation of estrogen receptor α through activation of proteasomes, *Mol. Cell. Biol. 23*, 1843−1855.
17. Ohtake, F., Takeyama, K.-I., Matsumoto, T., Kitagawa, H., Yamaoto, Y., Nohara, K., Tohyama, C., Krust, A., Mimura, J., Chambon, P., Yanaglsawa, J., Fujii-Kuriyama, Y., and Kato, S. (2003) Modulation of oestrogen receptor signalling by association with the activated dioxin receptor, *Nature 423*, 545−550.
18. Eftink, M. R., and Ghiron, C. A. (1976) Exposure of tryptophanyl residues in proteins. Quantitative determination by fluorescence quenching studies, *Biochemistry 15*, 672−680.
19. Sreerama, N., and Woody, R. W. (2000) Estimation of protein secondary structure from CD spectra: Comparison of CONTIN, SELCON and CDSSTR methods with an expanded reference set, *Anal. Biochem. 287*, 252−260.
20. Whitmore, L., and Wallace, B. A. (2004) DICHROWEB, an online server for protein secondary structure analyses from circular dichroism spectroscopic data, *Nucleic Acids Res. 32*, W668−W673.

21. Tora, L. (2002) A unified nomenclature for TATA box binding protein (TBP)-associated factors (TAFs) involved in RNA polymerase II transcription, *Genes Dev. 16*, 673−675.
22. Swanson, H. I., and Yang, J. H. (1998) The aryl hydrocarbon receptor interacts with transcription factor IIB, *Mol. Pharmacol. 54*, 671−677.
23. Rojo-Niersbach, E., Furukawa, T., and Tanese, N. (1999) Genetic dissection of hTAF(II)130 defines a hydrophobic surface required for interaction with glutamine-rich activators, *J. Biol. Chem. 274*, 33778−33784.
24. Choi, Y., Asada, S., and Uesugi, M. (2000) Divergent hTAFII31-binding motifs hidden in activation domains, *J. Biol. Chem. 275*, 15912−15916.
25. Kumar, M. B., Tarpey, R. W., and Perdew, G. H. (1999) Differential recruitment of coactivator RIP140 by Ah and estrogen receptors. Absence of a role for LXXLL motifs, *J. Biol. Chem. 274*, 22155−22164.
26. Baskakov, I. V., Kumar, R., Srinivasan, G. J. Y. S., Bolen, D. W., and Thompson, E. B. (1999) Trimethylamine *N*-oxide-induced cooperative folding of an intrinsically unfolded transcription-activating fragment of human glucocorticoid receptor, *J. Biol. Chem. 274*, 10693−10696.
27. Kumar, R., Lee, C., Bolen, D. W., and Thompson, E. B. (2001) The conformation of the glucocorticoid receptor AF1/tau1 domain induced by osmolyte binds co-regulatory proteins, *J. Biol. Chem. 276*, 18146−18152.
28. Reid, J., Kelly, S. M., Watt, K., Price, N. C., and McEwan, I. J. (2002) Conformational analysis of the androgen receptor amino-terminal domain involved in transactivation. Influence of structure-stabilizing solutes and protein−protein interactions, *J. Biol. Chem. 277*, 20079−20086.
29. Kumar, R., Betney, R., Li, J., Thompson, E. B., and McEwan, I. J. (2004) Induced α-helix Structure in the AF1 of the Androgen Receptor Upon Binding the Transcription Factor TFIIF, *Biochemistry 43*, 3008−3013.
30. Jones, L. C., and Whitlock, J. P., Jr. (2001) Dioxin-inducible transactivation in a chromosomal setting. Analysis of the acidic domain of the Ah receptor, *J. Biol. Chem. 276*, 25037−25042.
31. Wright, P. E., and Dyson, H. J. (1999) Intrinsically unstructured proteins: Re-assessing the protein-structure function paradigm, *J. Mol. Biol. 293*, 321−331.
32. Metz, R., Banister, A. J., Sutherland, J. A., Hagemeier, C., O'Rourke, E. C., Cook, A., Bravo, R., and Kouzarides, T. (1994) c-Fos-induced activation of a TATA-box-containing promoter involves direct contact with TATA-box-binding protein, *Mol. Cell. Biol. 14*, 6021−6029.
33. Kalkhoven, E., Valentine, J. E., Heery, D. M., and Parker, M. G. (1998) Isoforms of steroid receptor co-activator 1 differ in their ability to potentiate transcription by the oestrogen receptor, *EMBO J. 17*, 232−243.
34. Chen, D., Ma, H., Hong, H., Koh, S. S., Huang, S. M., Schurter, B. T., Aswad, D. W., and Stallcup, M. R. (1999) Regulation of transcription by a protein methyltransferase, *Science 284*, 2174−2177.
35. Kumar, M. B., and Perdew, G. H. (1999) Nuclear receptor coactivator SRC-1 interacts with the Q-rich sub-domain of the AhR and modulates its transactivation potential, *Gene Expression 8*, 273−286.
36. Reid, J., Murray, I., Watt, K., Betney, R., and McEwan, I. J. (2002) The androgen receptor interacts with multiple regions of the large subunit of general transcription factor TFIIF, *J. Biol. Chem. 277*, 41247−41253.
37. Bevan, C. L., Hoare, S., Claessens, F., Heery, D. M., and Parker, M. G. (1999) The AF1 and AF2 domains of the androgen receptor interact with distinct regions of SRC1, *Mol. Cell. Biol. 19*, 8383−8392.
38. Christiaens, V., Bevan, C. L., Callewaert, L., Haelens, A., Verrijdt, G., Rombauts, W., and Claessens, F. (2002) Characterisation of the two coactivator-interacting surfaces of the androgen receptor and their role in transcriptional control, *J. Biol. Chem. 277*, 49230−49237.
39. Beischlag, T. V., Wang, S., Rose, D. W., Torchia, J., Reisz-Porszasz, S., Muhammad, K., Nelson, W. E., Probst, M. R., Rosenfeld, M. G., and Hankinson, O. (2002) Recruitment of the NCoA/SRC-1/p160 family of transcriptional coactivators by the aryl hydrocarbon receptor/aryl hydrocarbon receptor nuclear translocator complex, *Mol. Cell. Biol. 22*, 4319−4333.
40. Wang, S., and Hankinson, O. (2002) Functional involvement of the Brahma/SWI2-related gene 1 protein in cytochrome P4501A1 transcription mediated by the aryl hydrocarbon receptor complex, *J. Biol. Chem. 277*, 11821−11827.
41. Nguyen, T. A., Hoivik, D., Lee, J. E., and Safe, S. (1999) Interactions of nuclear receptor coactivator/corepressor proteins with the aryl hydrocarbon receptor complex, *Arch. Biochem. Biophys. 367*, 250−257.
42. Tian, Y., Ke, S., Chen, M., and Sheng, T. (2003) Interactions between the aryl hydrocarbon receptor and P-TEFb, *J. Biol. Chem. 278*, 44041−44048.
43. Emami, K. H., and Carey, M. (1992) A synergistic increase in potency of a multimerised VP16 transcriptional activation domain, *EMBO J. 11*, 5005−5012.
44. Sauer, F., Hansen, S. K., and Tjian, R. (1995) DNA template and activator-coactivator requirements for transcriptional synergism by *Drosophila* Bicoid, *Science 270*, 1825−1828.
45. Combet, C., Blanchet, C., Geourjon, C., and Deleage, G. (2000) NPS@: Network protein sequence analysis, *Trends Biochem. Sci. 25*, 147−150.

BI0487701